CRYSTALLINE SILICON PHOTOVOLTAIC MODULES PERFORMANCE INVESTIGATION

Dhass. AVITHI.DESAPPAN
Department of Mechanical Engineering, Anna University, Chennai-600025, India.
dasaradhan.ad@gmail.com

Lakshmi.PONNUSAMY
Department of Electrical and Electronics Engineering, Anna University, Chennai-600025, India.
p_lakshmi@annauniv.edu

Natarajan.ELUMALAI
Department of Mechanical Engineering, Anna University, Chennai-600025, India.
enat123@gmail.com

Abstract: *The crystalline silicon is categorized into mono-crystalline (m-Si) and poly-crystalline (p-Si) photovoltaic cells. These two types of solar cells differ in their performance parameters, due to their structure, internal property, temperature co-efficient, and loss in power output. In this paper, an analysis has been carried out by comparing the performance of m-Si and p-Si when connected in series or parallel or in combination. The variations in fill factor and efficiency due to changes in the electrical load resistance, and the mismatch effect on electrical parameters have been studied. Under different climatic conditions, m-Si and p-Si performance may differ and therefore the suitable area of selection varies, based on the type of solar cell used. Two p-Si and one m-Si photovoltaic module exhibits 80.51% fill factor early in the day and 11.25% fill factor during the latter part of the day. The fill factor Vs load resistance curve for various combinations and photovoltaic module efficiency Vs photovoltaic module area curve are drawn at T_1 time period. The performance of the photovoltaic modules are evaluated from output characteristic curves of voltage, current, and power with tilt angle.*

Key words: *monocrystalline, polycrystalline, fill factor, efficiency, electrical resistive load, tilt angle.*

1. Introduction

Present world economics and industrial growth level are purely related to the amount of energy generated in a particular country. In developing countries, such as India, the growth of automobile industries or that in the level of agricultural produce does not meet the associated demand for these commodities. This is mainly because of the difference in the level of energy generated and consumed. This problem may be overcome by increasing solar photovoltaic (SPV) power generation, which leads to quality power generation at low costs and has countless benefits. The manufacturing cost of monocrystalline silicon (m-Si) is higher than that of polycrystalline silicon (p-Si). It is crucial to reduce the initial investment cost and to increase the amount of energy generated. Combining the m-Si and p-Si modules leads to the generation of sufficient levels of energy with the least amount of investment. These PV module combinations can be installed under normal and high irradiation (desert climate) climatic conditions. SPV modules constitute silicon, copper indium diselenide, gallium-arsenide etc. The use of silicon in SPV module manufacturing is a new technique adopted to develop modules in bulk. A crystalline semiconductor has a higher density, absorbs more solar radiations, and has a longer life. The overall performance of such semiconductor materials depends on light absorption, energy conversion efficiency, and material synthesizing technology [1-3]. A solar cell may not able to supply maximum possible power output at all conditions. It is proceed to implement the fuzzy and neuro-fuzzy techniques to overcome this kind of problem [4].

With exposure to average solar radiation per day, polycrystalline modules exhibit higher power output efficiency than m-Si modules. The power output of m-Si and amorphous silicon (a-Si) modules drops at high temperatures. The a-Si modules exhibit high

power output efficiency at low solar radiation [5]. m-Si modules exhibit higher performance characteristics, such as fill factor, power conversion efficiency, and energy efficiency, than p-Si modules at 200–500 W/m^2 irradiance. The series resistance is higher in the p-Si modules than in the m-Si modules. In both PV modules, open circuit voltage and short circuit current decreases with an increase in temperature [6]. The energy conversion rate of crystalline modules is higher (12%–17%) than that of amorphous silicon (a-Si) modules (4%–6%).

In summer, the efficiency of a-Si and p-Si modules decreases up to 5% compared with that of m-Si modules (up to 10%)[7]. The m-Si modules exhibit highest efficiency among the silicon-based PV modules (16%–24%). The p-Si modules produce 14%–18% efficiency [8]. Typical m-Si modules are usually 125 × 125 mm or longer and are pseudo-square shaped. Similarly, p-Si modules are usually 100 × 100 mm or longer and are square shaped [9]. The temperature coefficient for the m-Si and p-Si modules was approximately −0.4 V/°C. In practice, both PV technologies may not have the same value [10]. Solar radiation reduces with a change in the position of PV modules. The tilt angle is a major parameter for determining output performance. Change in the tilt angle depends on the site specification and the daily, monthly, and yearly solar radiation path of the sun [11]. During winter, in South Africa, a PV panel with a tilt angle between 26° and 36° produces optimal power output [12]. The degradation rate (%/year) and power output loss of crystalline PV modules are lower than those of other PV modules [13]. Under standard temperature conditions (STC), the PV module parameters may vary at different locations for the m-Si modules compared with silicon film and triple-junction amorphous modules [14]. The p-Si modules are of lower costs and have higher power conversion efficiency than m-Si modules. The p-Si technology is best suited for SPV modules, whereas m-Si technology is tedious and its temperature level has to be maintained within limits for better efficiency [15]. Polycrystalline modules under outdoor operating conditions lose 31% efficiency, 18% power output, and 18% fill factor compared with those under STC indoors[16].

The fill factor decreases with an increase in solar irradiation from 0.1 sun (%) to 1 sun (%). The fill factor decreases from 0.6 to −2.3 with an increase in temperature at 1 sun (%) from 65°C to 95°C. Similarly, the fill factor increases from −0.7 to 0.1 with an increase in temperature at 0.1 sun (%). Performance factors mainly depend on the solar irradiation of PV modules and the corresponding temperature variation. The PV modules affect the temperature-related problem considerably and eventually degrade the performance [17]. The m-Si modules provide slightly higher current efficiency than p-Si modules. The efficiency of the m-Si and p-Si modules differs because of variations in their manufacturing techniques. This deviation can be observed only during the peak hours of solar irradiation. These effects are identified under semi-arid climate conditions and may also be identified during completely sunny days [18]. The shunt resistance of SPV modules affects the fill factor and power output [19]. During summer, the tilt angle is maintained at15° (±2.5°) in Athens. This tilt angle was established using a theory based on solar geometric equations [20]. The PV module performance was affected by a change in the orientation and tilt angle with respect to the horizontal plane. The efficiencies of the rotating and fixed types of PV modules were compared. A 28.76% increase was observed in the solar irradiation of the rotating-type PV modules, which resulted in 24.78% increased power [21]. Temperature has a higher impact on m-Si modules than on p-Si and thin-film SPV modules. The efficiency of the m-Si and thin-film SPV modules decreases by 15% and 5%, respectively [22]. Therefore, a region experiencing high solar irradiation may not exhibit a higher performance of the m-Si modules than of the p-Si modules.

In this study, the p-Si modules exhibit a superior fill factor than the m-Si modules because the m-Si modules are highly influenced by temperature. In the past, a comparative analysis of the m-Si and p-Si modules was conducted. The performance of the newly combined m-Si and p-Si modules as a single panel was analysed extensively under different electrical load conditions and with different PV module combinations. The fill factor and efficiency of various PV module combinations were calculated. The angle of inclination considered for the study ranged from 5° to 50°, with the surface plane. It causes a change in the output voltage and current of a PV panel. The PV panel consisted of two m-Si and p-Si modules, and these modules were connected diagonally to the PV panel.

2. Basics of PV modules

2.1 SPV module equivalent circuit

Figure.1 displays the SPV module equivalent circuit diagram. When solar radiation falls on PV modules, light current (I_L) is generated and diode current (I_D) increases gradually. The SPV modules have two parasitic resistances: shunt and series components. They can be connected in parallel and series across the load circuits.

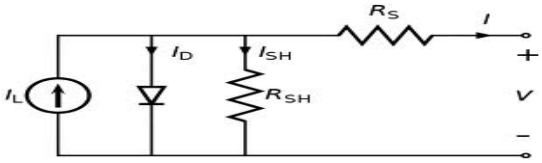

Fig. 1. Solar cell Equivalent Circuit [19].

The current generated in PV modules [7, 23-24] is calculated using the following equations:

$$I = I_L - I_D - \frac{V + IR_s}{R_{sh}} \tag{1}$$

$$I = I_L - I_0\left(\exp\left(\frac{q(V + IR_s)}{NKT} - 1\right) - \frac{V + IR_s}{R_{sh}}\right) \tag{2}$$

$$I = I_L - I_0\left[\exp\left(\frac{\beta(V + IR_s)}{N} - 1\right) - G^*(V + IR_s)\right] \tag{3}$$

The light-generated current (Khan F, et al.,(2010)) is calculated using the following equation:

$$I_L = (I_{scr} + k_i(I_c + 273.15 - T_r)) \times G \tag{4}$$

2.2 SPV Two diode model

It consists of two diodes, which are connected in parallel with current sources as shown in fig 2. These two diodes are used to rectify and modelling of space charge recombination current towards the controlling of shunt resistor path or leakage current path. This model is most suitable for low radiation conditions but under varying temperature conditions not able to obtain the dynamic resistance of a solar cell. This problem is associated with single diode model with varying temperature conditions [25-26].

In general, single diode model of solar cell is most suitable for hot climatic conditions like India. In this paper, we considered single diode of solar cell to investigate the characteristic parameters instead of two diode model of solar cell [27].

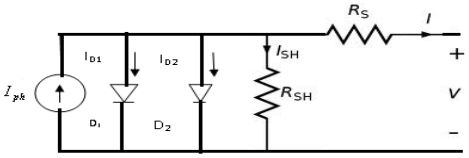

Fig 2. Equivalent circuit of a double diode model of a solar cell [25].

$$I_L = I_{ph} - I_{D1} - I_{D2} - I_{sh} \tag{5}$$

and

$$I_L = \left\{\begin{array}{l} I_{ph} - I_{SD1}\left[\exp\left(\frac{q(V_L + I_L R_S)}{N_1 KT}\right) - 1\right] \\ - I_{SD2}\left[\exp\left(\frac{q(V_L + I_L R_S)}{N_2 KT}\right) - 1\right] \\ - \left[\frac{V_L + I_L R_S}{R_{sh}}\right] \end{array}\right\} \tag{6}$$

The total global irradiation [20] splits into three forms of radiation waves when it falls on a PV panel: direct radiation (S), diffuse radiation (D_β), and reflective radiation (R_β).

$$G_\beta = S + D_\beta + R_\beta \tag{7}$$

Among these radiation waves, direct radiation is useful for generating electrical energy, and other radiations are dissipated into the atmosphere in the form of heat. The amount of energy received from the sun under the above atmospheric or extraterrestrial conditions is calculated using the empirical formulae given below [11].

$$I_{ext} = I_{sc}[1.0 + 0.333\cos(360 * n/365)] \tag{8}$$

The fill factor is a parameter for measuring the quality of PV modules. Its value ranges from 0 to 1. The fill factor[24] values for the m-Si and p-Si modules are given in Table 1.

$$P_m = V_m I_m = (FF) V_{oc} I_{sc} \tag{9}$$

$$FF = \left(\frac{I_m V_m}{I_{sc} V_{oc}}\right) \tag{10}$$

The SPV Efficiency [28] is used to measure or identify the energy conversion rate from solar irradiation to the electrical energy output. The power to area ratio is high for the m-Si modules and low for the p-Si modules. These details are given in

Table 1.

$$\eta_{\max} = \left(\frac{I_m V_m}{I_T A_c}\right) = \left(\frac{(FF) I_{sc} V_{oc}}{I_T A_c}\right) \qquad (11)$$

Table 1 presents the electrical parameters and area requirements, suitable climatic conditions, shape of PV modules, power to area ratio, and colour suitability for the m-Si and p-Si modules. Table 3 presents experimental values such as open circuit voltage, short circuit current, rated power, maximum voltage, and maximum current. Here, the specifications of the m-Si and p-Si modules are same, but the modules differ in size and colour.

2.3 m-Si and p-Si PV modules

The electrical resistivity of m-Si modules is lower than that of p-Si modules, and the electrical resistivity of the p-Si modules is only half of that of the m-Si modules at 298 K [29]. In addition to the basic differences between the m-Si and p-Si modules, the m-Si modules tend to produce a lower de-rating coefficient at higher temperatures than other technologies. The p-Si modules have a better de-rating coefficient at high temperatures [30]. The electrical and physical properties of m-Si and p-Si PV modules are given in Table 1. The m-Si and p-Si modules may not be a suitable option under all climatic conditions. The m-Si modules are more expensive than the p-Si modules. Other comparison parameters are listed in Table 1. The hybrid system consisting m-Si and p-Si modules in a single module was developed by Panasonic hybrid panels. This system leads to improved performance and can be used for more limited roof areas [31].

3. Experimental Set up

A solar kit consisting the PV panel, irradiance sensor, temperature sensor, resistive load, voltmeter, and ammeter measuring devices is shown in Fig. 3.

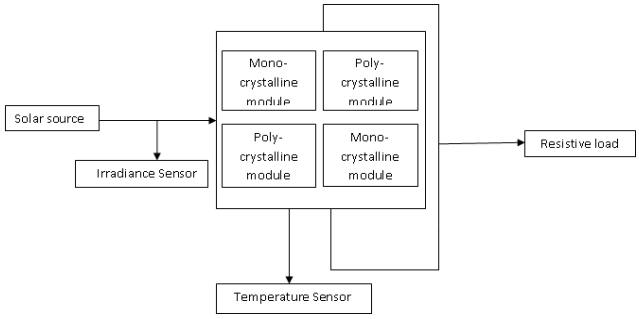

Fig. 3. Block Diagram for measuring the performance parameters of Solar Photovoltaic Module.

The PV panel contains four PV modules: two m-Si and two p-Si modules. The m-Si and p-Si modules are placed diagonally. The PV modules may be connected in series, parallel, and combinations. The electrical characteristics of the m-Si and p-Si modules with 10 Wp-rated power are given in Table 2.

The PV panel consists of two different (m-Si and p-Si) PV modules. Solar irradiation was measured using a solar power meter and the input energy estimated for the PV panel. The outer surface temperature was measured using a thermometer. The experimental set up of the PV panel is shown in Figs. 4(a) and 4(b). The m-Si and p-Si modules are placed diagonally to each other and connected in series or parallel combinations. In the back view of SPV, the probe connection was either used to make an external connection with other PV modules or was connected to the load terminals. The output parameters were recorded across the electrical resistive load, which varies from 0–200 Ω.

Fig. 4(a) Photovoltaic module Experimental set up

Fig. 4(b) Back side view of solar photovoltaic panel.

Table 1 Properties of typical mono-crystalline and poly-crystalline solar cells [28, 32].

Type	color	Output voltage V_{oc} (V)	Output Current $J_{sc}(mA/cm^2)$	Fill factor (%)	Power to area ratio	Climate condition	Shape
m-Si	black	0.55-0.68	30-38	70-78	high	Good at cooler climates	square
p-Si	blue	0.55-0.65	30-35	70-76	Relatively less	Good at hotter zone	square

Table2. Electrical parameters of mono-crystalline and poly-crystalline PV modules [33].

Type	P_R (Wp)	Voltage (V)	V_{oc} (V)	Im (A)	I_{sc} (A)
m-Si/ p-Si module	10	16.4	21.0	0.61	0.7

3.1 Flow chart for experiments

The experimental procedure is outlined in Fig. 5 for measuring the performance parameters of SPV modules. The PV modules were connected through the different topologies (series and parallel connections). The PV panel was installed in an entirely sunny area, where the occupied areas were free from obstacles and shadowing problems. This system was connected with variable resistance (0–200 Ω) for different topologies. For various electrical resistances, the current and voltage were noted and tabulated, and the fill factor and efficiency were calculated at various time periods. This process was repeated for another connection scheme to get the best output from the PV system.

4. Results and Discussion

The various connection schemes of the m-Si and p-Si modules were placed under open air conditions to obtain electrical parameters. The voltage and current were measured for different resistive load values. These values were observed on 4th April, 2013 at 10:30 a.m. (T_1), 11:00 a.m. (T_2), 11:30 a.m. (T_3), and 12:00 p.m. (T_4). The fill factor and efficiency of the m-Si and p-Si modules are presented in Table 3. In addition, the corresponding solar radiation was measured at various time periods in a particular day. Various m-Si module combinations, which were connected in series, produced the maximum fill factor and efficiency. The same was observed with the p-Si modules. The remaining combinations, such as two m-Si and p-Si, two p-Si and one m-Si, and two m-Si and two p-Si modules connected in series and parallel for calculating the fill factor and efficiency are presented in Table 3. The combination of two p-Si and one m-Si modules connected in a parallel scheme exhibited maximum fill factor and efficiency in a particular day.

4.1 Single m-Si and p-Si module connection

Fig. 6 shows the fill factor and efficiency curves for different combination schemes. The electrical values were noted from the PV panel at 10:30 a.m. on 4th April, 2013. The variation in the fill factor values with load changes for the p-Si and m-Si modules is shown in Fig. 6(a). From the beginning to the end, the fill factor value was higher for the p-Si modules than for the m-Si modules. These changes in the performance curve were because of high solar irradiation on the surface of the PV modules.

The maximum fill factor values for the p-Si and m-Si modules were 0.33 and 0.44, respectively. The load resistance affects the output current from low to maximum resistance. The output current was low when the load was high. In addition, low loads produced low output current only up to a certain point. The point when a particular load maximizes the output current is called the critical point.

4.2 Two m-Si and p-Si modules connected in series

The parameters of two m-Si and two p-Si PV modules connected in series are displayed in Fig. 6(b). The fill factor values for the m-Si and p-Si modules were 0.62 and 0.71, respectively.

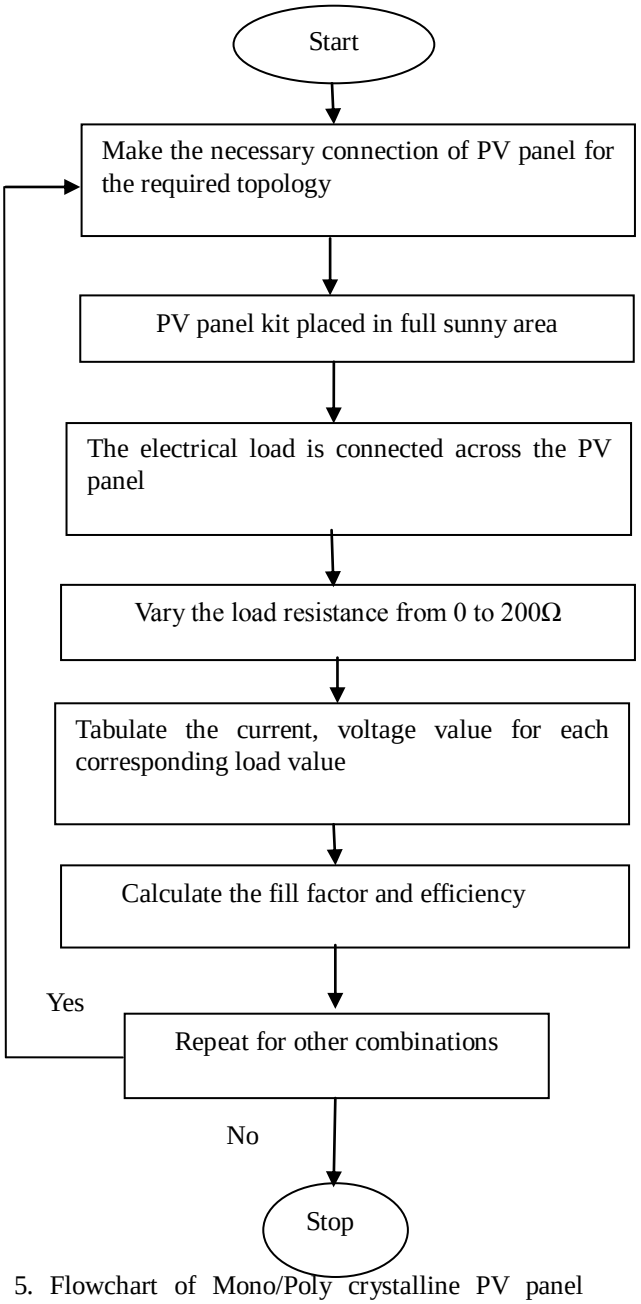

Fig 5. Flowchart of Mono/Poly crystalline PV panel performance parameter measurements.

These values were obtained under different climatic conditions and loads. Initially, the m-Si modules had a higher value than the p-Si modules. However, at the end, the p-Si and m-Si modules had attained the same value. At the critical point, the p-Si modules had a higher value than the m-Si modules. This change is due to higher solar irradiation of the p-Si modules.

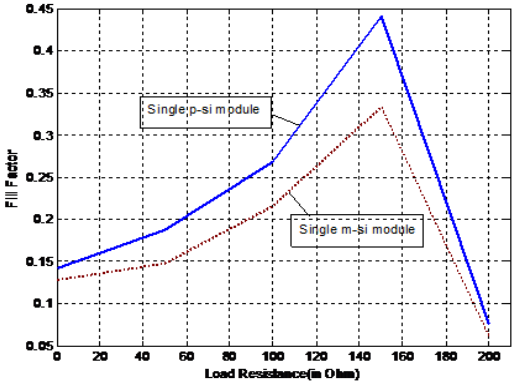

Fig 6(a). Single m-Si and p-Si module

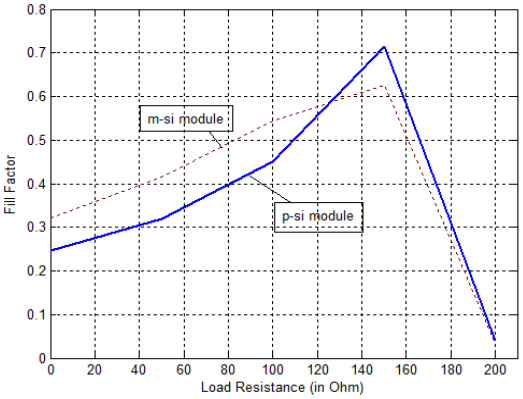

Fig 6(b). Two m-Si and p-Si module in series

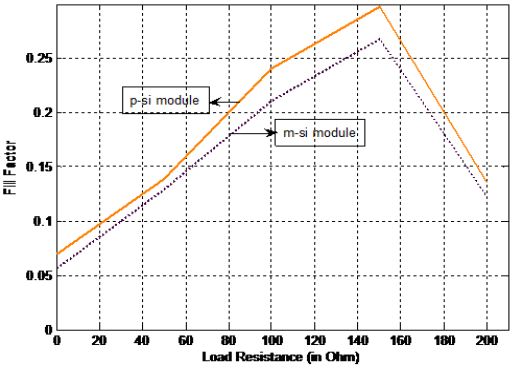

Fig 6(c).Two m-Si and p-Si module in paralle

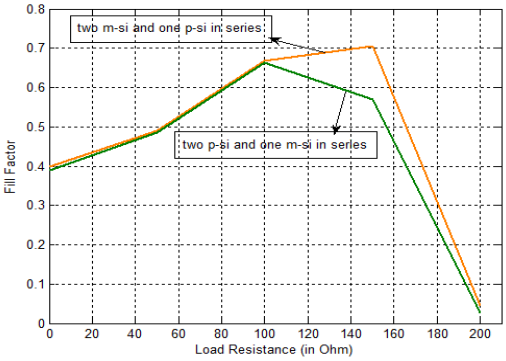

Fig 6(d). Combination of m-Si and p-Si module in series

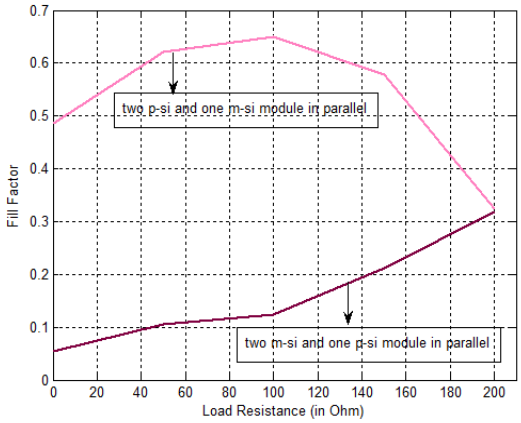

Fig 6(e). Combined m-Si and p-Si module in parallel

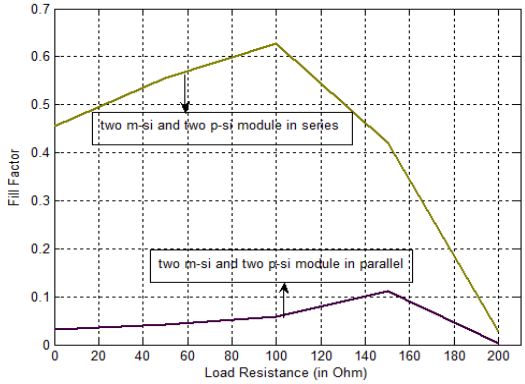

Fig 6(f).Combined two m-Si & p-Si module in series & parallel

The p-Si modules can absorb solar radiation and convert it to high electrical output. The aforementioned process showed slight deviation in case of m-Si modules.

4.3 Two m-Si and p-Si module in parallel connections

The fill factor performance curves for two m-Si and two p-Si modules in series connection are shown in Fig. 6(c). These curves are similar to the curves of single m-Si and p-Si module connection schemes. The fill factor values for the m-Si and p-Si modules were 0.27 and 0.29, respectively. On connecting the PV modules in parallel, the output current increased, but the voltage remained the same. At the same time, the fill factor decreased because of the p-Si module orientation.

4.4 Different combinations of p-Si and m-Si modules connected in series

The fill factor curves for two p-Si and one m-Si modules connected in series and for one p-Si with two m-Si modules connected in series are shown in Fig. 6(d). The fill factor values for the first and second combinations were 0.66 and 0.70, respectively. During high solar irradiation, the p-Si modules produced more electricity than the m-Si modules. Therefore, the p-Si modules are more suitable for hotter regions. The properties of the p-Si modules dominate those of m-Si modules. These two combinations had the same fill factor value until the critical point. After the critical point, the curve path changed because combined m-Si and p-Si orientation reduced the PV module structure, thereby reducing the electrical output current generation rate.

4.5 Different combinations of p-Si and m-Si modules connected in parallel

Performance curves for two p-Si and one m-Si modules and two m-Si and one p-Si modules connected in parallel combinations are shown in Fig. 6(e). The fill factor values for the two different combinations were vastly divergent. The fill factor values for the first and second combinations were 0.65 and 0.31, respectively. This was because m-Si combinations always reduce power production during high solar irradiation, and load resistance also reduces the output current.

4.6 Combinations of two m-Si and two p-Si modules connected in series and parallel

The fill factor curves for two m-Si and two p-Si modules in series and two p-Si and two m-Si modules in parallel are shown in Fig. 6(f). The fill factor values for the two PV modules in series and parallel combinations were 0.62 and 0.12, respectively. Therefore, an increase in the overall fill factor was observed. The main observation was that the fill factor values differed at the critical point. The major effect of a series connection was high output voltage from both PV modules. The efficiency versus area of PV modules for different m-Si and p-Si combinations with a change in the SPV module area at a time of T_1 from Table 3 is shown in Fig. 7. Two p-Si modules in series cause a 10.53% higher efficiency among all the other combinations, and this is possible only in summer. In general, m-Si combinations might produce maximum efficiency, but their internal structure are not capable of absorbing high amount of solar irradiation.

Table 3. Experimental data of fill factor and efficiency for different combinations of m-Si and p-Si modules.

S.No	PV Module Interconnection Scheme	T_1		T_2		T_3		T_4	
		FF (%)	η (%)	FF (%)	η (%)	FF (%)	η (%)	FF (%)	η (%)
1	Single m-Si module	33.40	4.44	22.88	3.03	39.20	5.11	37.64	4.82
2	Two m-Si module in series	67.50	8.04	58.65	6.98	68.66	8.41	61.60	7.08
3	Two m-Si module in parallel	26.80	4.20	21.05	3.15	25.85	3.81	23.29	3.37
4	Single p-Si module	44.16	6.61	42.81	6.42	40.50	5.91	44.06	6.44
5	Two p-Si module in series	71.53	10.53	61.06	9.00	67.86	9.82	62.35	8.87
6	Two p-Si module in parallel	29.81	4.60	24.98	3.86	26.57	4.03	29.44	4.38
7	Two m-Si and one p-Si module in series	70.63	9.31	69.68	9.20	67.46	8.74	70.91	9.32
8	Two m-Si and one p-Si module in parallel	37.85	4.35	68.15	9.34	35.16	4.73	31.64	4.17
9	Two p-Si and one m-Si module in series	66.41	9.85	62.15	9.23	65.31	9.51	66.53	9.52
10	Two p-Si and one m-Si module in parallel	64.97	9.24	66.00	9.37	80.51	11.25	68.52	6.77
11	Two p-Si and Two m-Si module in series	62.83	10.03	61.12	9.77	57.28	9.00	59.76	9.21
12	Two p-Si and Two m-Si module in parallel	11.14	1.86	37.57	6.58	31.06	5.34	43.92	9.41

This leads to decreased energy conversion. The combination of two m-Si and two p-Si modules in series produced the least efficiency of 1.869%. These efficiency changes are based on the load, climatic conditions, and selected PV module combinations.

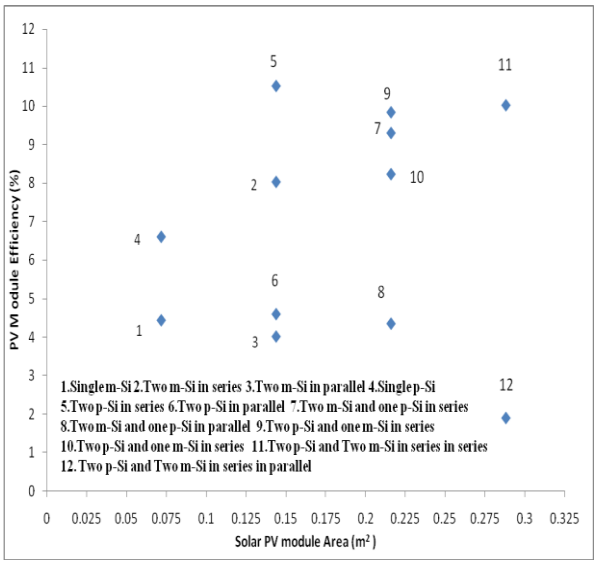

Fig 7. PV module efficiency for different combination of m-Si and p-Si modules.

4.7 Effects of tilt angle

The m-Si and p-Si modules were connected in series and parallel. The various tilt angle positions for optimal output voltage, current, and power were estimated at a particular point. The module output voltages for different tilt angles in parallel combinations are shown in Fig. 8. An optimal tilt angle of 10° produces the maximum output voltage of 14.1 V. As the tilt angle increases, the module output voltage decreases gradually. The module output current for different tilt angles in parallel combinations are given in Fig. 9. An optimal tilt angle of 5° produces a maximum current of 20.1 mA. In this configuration, the PV panel current decreases when the tilt angle increases. The module output voltage and current for different tilt angles in series combinations are presented in Figs. 10 and 11. A maximum output voltage of 78 V was produced, which was higher than the output voltage produced in a parallel combination. A maximum output current of 6.56 mA was attained, but it was lower than the output current obtained in a parallel combination.

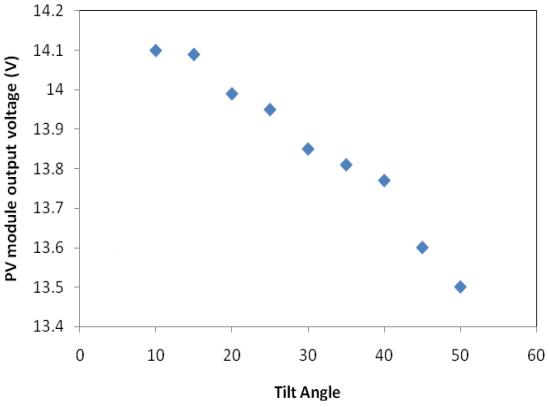

Fig 8. Comparison of PV Module Output Voltage (V) for various Tilt angle position in Parallel Combinations.

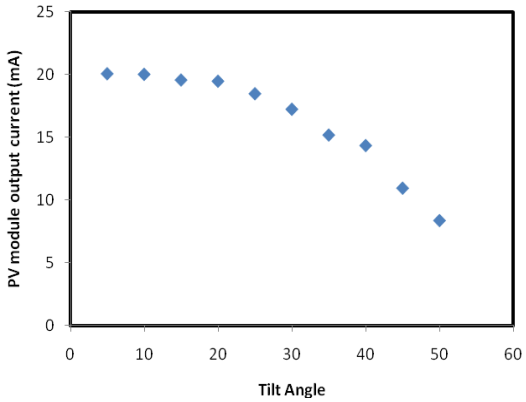

Fig 9. Comparison of PV module output current (mA) for various Tilt Angle position in Parallel Combinations

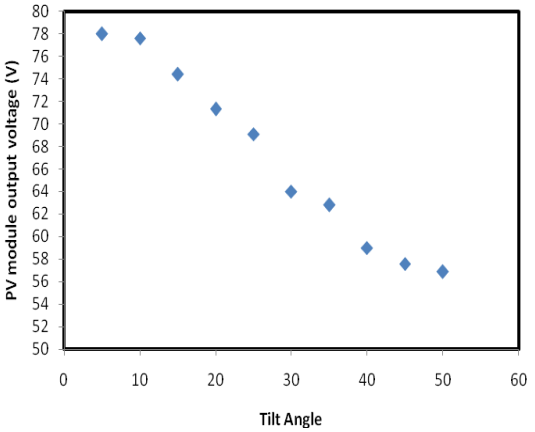

Fig 10. Comparison of PV Module Output Voltage (V) for various Tilt angle position in series Combinations.

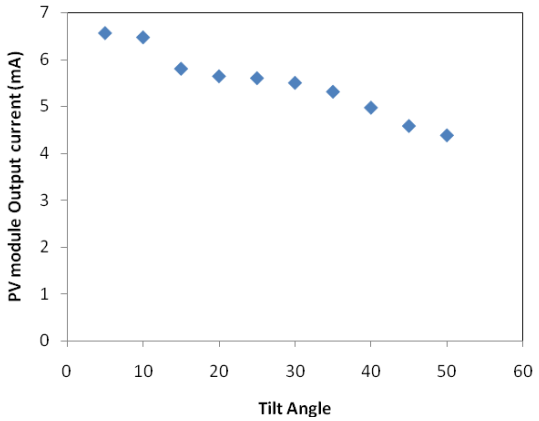

Fig 11. Comparison of PV module output current (mA) at various Tilt Angle position in series combinations

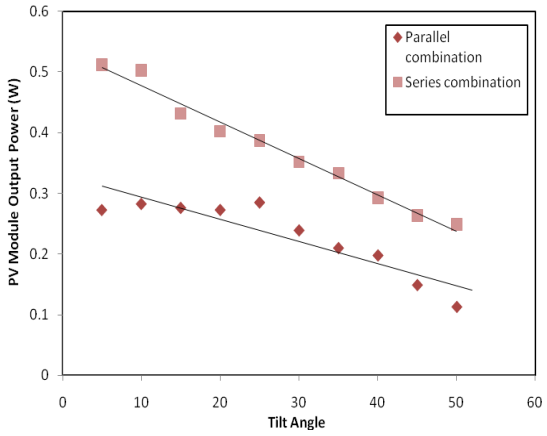

Fig 12. Comparison of PV module output power at various Tilt angle position for parallel and series combinations.

The PV module output power of both series and parallel combinations are shown in Fig. 12. A maximum output power of 0.511 and 0.285 W was attained in series and parallel combinations, respectively. The output of a series combination is linear and decreases with an increase in the tilt angle, because PV module output voltage in series greater than that in parallel. The output power curve for a parallel combination is not linear because the output current is not high.

5. Conclusions

An experimental investigation on the m-Si and p-Si panel was conducted in this study. This study was conducted to obtain short circuit current, open circuit voltage, fill factor, and efficiency. The following conclusions were drawn from the results of this study:

i. The m-Si modules produce the highest fill factor value under warm climatic conditions.
ii. The p-Si modules produced the highest fill factor value in a hot region or during sunny hours.
iii. The fill factor curves of the m-Si and p-Si modules show slight deviation, coinciding for the combinations of m-Si and p-Si modules.
iv. The fill factor values and efficiency deviated from the ideal conditions to practical conditions for various combinations of the m-Si and p-Si PV panels.
v. The same rating of the m-Si and p-Si module connections gave different performances, thus creating mismatch effects among them.
vi. The time (T_1) gave a maximum fill factor value and efficiency of 80.51 and 11.25%, respectively, during the test period.
vii. The series configuration (0.511 W) led to a better performance than the parallel configuration (0.285 W), because it generated a linear curve for the output power although the voltage and current varied gradually depending on the tilt angles.

Acknowledgements

The authors wish to thank Dr.Chetan Singh Solanki and MNRE (Ministry of New and Renewable Energy) providing the equipments through to do experimental work.

Nomenclature

$\beta = \frac{q}{KT}$ = Inverse thermal voltage.

η = Efficiency.

A_c = Area of the module (m^2).

FF = Fill factor.

G = Solar irradiance kW/m^2.

G_β = Total global irradiation.

$G^* = \frac{1}{R_{sh}} =$ Shunt conductance.

$I_L =$ Light-generated current (A).

$I_0 =$ Cell saturation of dark current (A).

$I_T =$ Incident solar irradiation $\left(W/m^2\right)$.

$I_m =$ Maximum output current (A).

$I_{scr} =$ Cell's short circuit current at 25˚C and $1 kW/m^2$.

$I_{sc} =$ Short circuit current (A).

$I_L =$ Terminal Current

$I_{ph} =$ Cell-generated photo current

$I_{D1}, I_{D2} =$ First and second diode current

$I_{SH} =$ Shunt resistance current

$I_{SD1}, I_{SD2} =$ First and second diode saturation current.

$K =$ Bolts man Constant (1.38×10^{-23} J/K).

$k_i =$ Cell's short circuit current co-efficient.

$N =$ Ideality factor.

n =day in a year.

$P_m =$ Output power (W).

P_R = Rated power (W_p).

$q =$ Electron charge $= 1.602 \times 10^{-19} C$.

$R_{sh} =$ Cell shunt Resistance (Ω).

R_s= Series Resistance (Ω).

$T =$ Cell's working temperature (K).

$T_r =$ Reference Temperature (K).

T_1= 10:30 AM.T_2=11:00 AM. T_3=11:30 AM. T_4=12:00AM.

$V_m =$ Maximum output voltage (V).

$V_{oc} =$ Open circuit voltage (V).

$W_p =$ Peak Watt.

References

1. Alberto Dolaro, George Cristian Lazaroiu, Sonia Leva, Gian Paolo Manzolini.,:*Experimental investigation of partial shading scenarios on PV(Photovoltaic) modules Energy*, LV, (2013), 466-475.
2. Shevaleevskiy.O,:*The future of solar photovoltaics; a new challenge for chemical physics*, Pure and applied chemistry, Vol: LXXX, (2008), pp:2079-89.
3. Oliva Mah, *Fundamentals of photovoltaic materials*, NSPRI (National Solar Power Research Institute Inc.); Dec 21st, 1998.
4. Zaghba, Terki N., Borni A., Bouchakour A., Benbitour Nee Khennane Messaouda,: *Adaptive Intelligent MPPT Controller Comparison of Photovoltaic system under different weather conditions of Ghardaia Site (South of Algeria)*, Journal of Electrical Engineering, Vol:XV, Edition:3, (2015).
5. AzhaR Ghazali M., Abdul Malek, Abdul Rahman, :*The performance of three different solar panels for solar electricity applying solar tracking device under the Malaysian climate condition*, Energy and Environmental Research, Vol.II, No.1,(2012).
6. Erden Cuce, Pinar Mert Cuce, Tulin Bali,:*An experimental analysis of illumination intensity and temperature dependency of photovoltaic cell parameters*, Applied Energy, Vol:CXI, (2013), pp: 374-382.
7. Bjorn Petter Jelle, Christer Breivik, Hilde Drolsum Rokenes :*Building integrated photovoltaic products: A state-of-the-art review and future research opportunities*, Solar Energy Materials and solar cells, Vol:C, (2012), pp: 69-96.
8. Marimuthu C., Kirubakaran V., : *Carbon pay back period for solar and wind energy project installed in india: A critical review*, Renewable and Sustainable Energy Reviews, *Vol:XXIII*, (2013) pp: 80-90.
9. Kanchan Vats, Vivek Tomar, Tiwari.G.N, :*Effect of packing factor on the performance of a building integrated semitransparent photovoltaic thermal (BISPVT) system with air duct*, Energy and Buildings, Vol:LIII, (2012), pp: 159-165.
10. Osalam shaltout M.A.M., El-hadad.A.A., Fadly M.A., Hassan A.F., Mahrous A.M.,: *Determination of suitable types of solar cells for optimal outdoor performance in desert climate*, Renewable Energy, Vol:XIX, (2000), pp: 71-74.
11. Osamede Asowata., James Swart., Chirsto Pienaar., :*Optimum tilt angles for photovoltaic panels during winter months in the vaal triangle, south Africa*, Smart Grid and Renewable Energy, Vol:III (2012), pp: 119-125.
12. John Kaaldellis., Dimitrios Zafirakis., :*Experimental investigation of the optimum photovoltaic panels' tilt angle during the summer period*, Energy, Vol: XXXVIII, (2012), pp: 305-314.
13. Hunter Fanney A., Mark W.Davis., Brian P/Dougherty., David L. king., William E.Boyson., Jay A. Kratochvil., :*Comparison of photovoltaic module performance measurements*, Journal of Solar Energy Engineering, Vol.CXXVIII, May (2006), pp: 152-159.

14. Tyagi V.V, Nurul A.A. Rahim, N.A.Rahim, JeyrajA. /Selvaraj.L, *Progress in solar PV technology: Research and achievements*, Renewable and Sustainable Energy Review, Vol: XX, (2013), pp: 443-461
15. Agroui K, *Indoor and outdoor characterizations of photovoltaic module based on multicrystalline solar cells*, Energ Procedia, Vol: XVIII, (2012), pp: 857-866.
16. Abdelkader M.R, Al-Saleymeh.A, Al-Hamamre.Z, Firas Sharaf, *A comparative analysis of the performance of mono crystalline and multicrystalline PV cells in semiarid climatic condition: the case of Jordan*, Jordan Journal of Mechanical and Industrial.Engineering, Vol.IV, No.5, (2010), pp; 543-552.
17. Amit Kumar Yadav, Chandel.S.S, *Tilt angle optimization to maximize incident solar radiation : A review*, Renewable and sustainable energy review,Vol:XXIII (2013), pp: 503-513.
18. "*Typical Climate Data for Selected Radiation Stations*", Solar Radiation Hand Book (2008), Solar Energy Centre, MNRE, Indian Metrological Department, pp.3-5.
19. Dhass A.D., Natarajan E., Ponnusamy L., :*Influence of shunt resistance on the performance of solar photovoltaic cell*, Emerging Trends in Electrical Engineering and Energy Management (ICETEEM), 2012 International Conference on, pp 382-386.
20. Pavlovic.T, Pavlovic.Z, Pantic.L, Kpstic.L.J, *Determining optimum tilt angles and orientations of photovoltaic panels NIS Serbia*, Contemporary Materials, (2012), pp:1-2.
21. Ying-Pin Chang, *Optimal the tilt angles for photovoltaic modules in Taiwan*, International Journal of Electrical Power and Energy Systems. Vol: XXXII, (2010), pp: 956-964.
22. Vikrant Sharma, S.S. Chandel, *Performance and degradation analysis for long term reliability of solar photovoltaic system*: A review, Renewable and Sustainable Energy Review, Vol:XXVII, (2013), pp: 753-767.
23. Khan F, Singh S.N, Husain M, *Effect of light intensity on module parameters of a silicon solar module*, Solar Energy Materials and Solar cells, Vol: XCIV, (2010), pp: 1473-6.
24. Nancy Jiang, Taro Sumitomo, Timothy Lee, Alba Pellaroque, Oliver Bellon, Damion Milliken, Hans Desilvestro:*High temperature stability of dye solar cells*, Solar Energy Materials and Solar cells, Vol :CXIX, Dec 2013, pp: 36-50.
25. AlRashidi M.R., El-Naggar K.M., Alhajri M.F.,: Parameters Estimation of double diode solar cell model, International Journal of Electrical, Computer, Energitic, Electronic and Communication Engineering, Vol:VII, No:2, (2013).
26. Ritesh Dash, S.M.Ali, " Comparitive study of one and two diode model of solar photovoltaic cell", International Journal of Research in Engineering and Technology Vol:III, Issue: 10, Oct-2014.
27. Basim Alsayid, " Modeling and Simulation of Photovoltaic cell/module/array with two diode model", International Journal of Computer Technology and Electronics Engineering, Vol: I, Issue 3, June 2012.
28. Solanki .C.S, Subarto kumar Ghosh, Mohammad Hasanuzzaman shawon, Ashifur Rahman, Rifat Abdullah, *Modelling of PV arrays and analysis of different parameters*, International Journal of Advancement in Research & Technology, Vol II, Issue5, May-2013.
29. McLEOD A.D, Haggerty.J.S, Sadoway D.R, *Electrical resistivity of monocrystalline and polycrystalline* TiB_2, Journal of American Ceramic Society, Vol.LXVII, No.11, November 1984.
30. *Solar technology*, (online) available from <http: www.wbbcc.wordpress.com/2010/08/solar-technology-explained.pdf>, (accessed on 22nd June 2015).
31. *Solarphotovoltaic/pvtechnology*(online)available from<http:www.horizonrenewable.org/solar-photovoltaics/pv-technology-types/> (accessed on 25th June 2015).
32. Monocrystalline or polycrystalline solar panek (online) available from <http:www.sustainable .com.au/> (accessed on 16th September 2015).
33. *Performance parameters of monocrystalline / poly crystalline module* (online) available from <http:www.thriveenergy.co.in/> (accessed on 06th August, 2015).